

Implicit Corotational Method: FEM implementation

Giovanni Garcea¹, Antonio Madeo¹, Giuseppe Zagari¹, Emira Lanari¹

¹ *Dipartimento di modellistica per l'ingegneria, University of Calabria, Italy*

E-mail: giovanni.garcea@unical.it, antoniomadeo@labmec.unical.it, gzagari@unical.it

Keywords: Implicit Corotational Method, Total Lagrangian and Corotational mixed finite elements, nonlinear Saint Venánt 3D beam and Kirchoff thin plate, path-following and asymptotic analyses.

SUMMARY. The **Implicit Corotational Method (ICM)** is a powerful and consolidated approach for recovering objective and suitable for FEM implementation nonlinear models fully reusing the corresponding linear ones [1, 2]. An appropriate stress/strain (Biot) representation for the description of the nonlinear elastic continuum, the use of corotational algebra for splitting the body motion into rigid and deformative parts and some assumptions on the reinterpretation of linear theory in the nonlinear context, constitute the basis of the ICM.

An important feature of the method is the possibility of obtaining a tool that allow an easy FEM implementation. Different kinds of interpolation strategies (Total and Updated Lagrangian, Corotational) are used within the approach. A standard format and an automated way of implementing the nonlinear models into the FEM context based on the use of algebraic manipulator and aimed at path-following or asymptotic analyses have been developed [3].

The FEM implementation is provided for 3D beam and plate models recovered using ICM. For the 3D beam model, based on Saint Venánt theory [2], the assumptions about the rotation parameters and the details on handling finite rotations are given clearly. The accuracy of some mixed finite elements that differ for the interpolation laws assumed for the kinematics and statics fields and for the interpolations strategy is pointed out. For the thin plate model, based on Kirchoff hypothesis [1], the proposed finite element is implemented as specialized one in asymptotic FEM code (see [7]).

A numerical investigation has been performed, also comparing beam and plate based solutions in the case of thin-walled beams. The good agreement between the recovered results with the theoretical ones and the numerical benchmarks, shows clearly the correctness and capability of the proposed approach for numerical implementations.

1 IMPLICIT COROTATIONAL METHOD: BASIC ITEMS

The goal of the **Implicit Corotational Method (ICM)** is to reuse the results of linear theories in nonlinear context in order to obtain objective structural models (e.g. beam, shell) which are suitable for FEM implementations. An appropriate stress/strain representation for the description of the nonlinear elastic continuum, the use of corotational algebra for splitting the body motion into the rigid and deformative parts and some assumptions about the reinterpretation of linear theory in the nonlinear context, constitute the basis of the ICM. The basic items of the method are summarized in this section while for a more detailed discussion the reader can refer to [2].

1.1 Some continuum mechanics

The nonlinear elastic continuum is described using Biot stress σ_b and strain ε_b , so in mixed form, strain energy is expressed as:

$$\Phi[\sigma_b, \varepsilon_b] := \int_V \left\{ \sigma_b \cdot \varepsilon_b - \frac{1}{2} \sigma_b \cdot C \sigma_b \right\} dV \quad (1a)$$

C being the bilinear compliance operator defining the constitutive law, so that the ICM is assumed to be equal to that of the linear continuum and being V the volume of the body in the undeformed reference configuration. Through a corotational (CR) frame defined by a rotation tensor \mathbf{Q} with respect to the global fixed frame $\{\mathbf{e}_1, \mathbf{e}_2, \mathbf{e}_3\}$ and using the polar decomposition theorem, the Biot strain can be expressed in CR frame as:

$$\varepsilon_b := \mathbf{U} - \mathbf{I} = \mathbf{R}^T \mathbf{F} - \mathbf{I} = \bar{\mathbf{R}}^T \bar{\mathbf{F}} - \mathbf{I}, \quad \bar{\mathbf{F}} = \mathbf{Q}^T \mathbf{F}, \quad \bar{\mathbf{R}} = \mathbf{Q}^T \mathbf{R} \quad (1b)$$

where we have denoted quantities in CR frame with a bar and being \mathbf{F} is the deformation gradient, \mathbf{U} the right stretch tensor and \mathbf{R} the polar decomposition rotation. Assuming, in the CR frame, the polar decomposition rotation $\bar{\mathbf{R}}$ to be small and relating it with the skew-symmetric $\bar{\mathbf{W}}$ part of the gradient of displacements $\nabla \bar{\mathbf{u}} = \bar{\mathbf{F}} - \mathbf{I}$ we have:

$$\bar{\mathbf{R}} \approx \mathbf{I} + \bar{\mathbf{W}} \quad (1c)$$

With some algebra the following quadratic expression for Biot strain is obtained:

$$\varepsilon_b \approx \bar{\mathbf{E}} + \frac{1}{2} (\bar{\mathbf{E}}\bar{\mathbf{W}} - \bar{\mathbf{W}}\bar{\mathbf{E}} - \bar{\mathbf{W}}\bar{\mathbf{W}}), \quad \bar{\mathbf{E}} := \text{sym}[\nabla \bar{\mathbf{u}}], \quad \bar{\mathbf{W}} := \text{skew}[\nabla \bar{\mathbf{u}}] \quad (1d)$$

When $\bar{\mathbf{W}} = \mathbf{0}$, it holds that Biot strain is equal to linear strain tensor $\varepsilon_b = \bar{\mathbf{E}}$. Therefore the, Biot stress/strain representation appears to be the most appropriate representations for recovering linear solutions.

1.2 Reuse of linear solutions in nonlinear context

Linear solutions, when structured continua (e.g. beam, shell) are considered, provide in general the stress field $\bar{\boldsymbol{\sigma}}[\mathbf{t}]$ in terms of global stress parameter \mathbf{t} and the gradient of displacement $\nabla \bar{\mathbf{u}}[\bar{\mathbf{d}}] = \bar{\mathbf{E}}[\bar{\mathbf{d}}] + \bar{\mathbf{W}}[\bar{\mathbf{d}}]$ in terms of global kinematics parameter $\bar{\mathbf{d}}$. The ICM assumes that Biot stress $\boldsymbol{\sigma}_b$ is equal to the linear stress tensor and that Biot ε_b is evaluated, in an appropriate CR frame, using quadratic formula (1d) in which the gradient of displacements is evaluated from linear solutions:

$$\boldsymbol{\sigma}_b \equiv \bar{\boldsymbol{\sigma}}[\mathbf{t}], \quad \bar{\mathbf{E}} \equiv \bar{\mathbf{E}}[\bar{\mathbf{d}}], \quad \bar{\mathbf{W}} \equiv \bar{\mathbf{W}}[\bar{\mathbf{d}}] \quad (2)$$

In the frame of a Galerkin approximation, the mixed energy (1) can be rewritten in terms of the global stress and kinematics parameters \mathbf{t} and $\bar{\mathbf{d}}$:

$$\Phi[\mathbf{t}, \boldsymbol{\varrho}] = \int_s \left\{ \mathbf{t}^T \boldsymbol{\varrho}[\bar{\mathbf{d}}] - \frac{1}{2} \mathbf{t}^T \mathbf{H} \mathbf{t} \right\} ds \quad (3)$$

where $\boldsymbol{\varrho}[\bar{\mathbf{d}}]$ is the deformation work-conjugate with \mathbf{t} , \mathbf{H} a compliance operator and s an appropriate abscissa describing the structured continuum. The relationships between kinematical parameter $\bar{\mathbf{d}}$ in CR frame and \mathbf{d} in fixed frame complete the kinematics. When $\bar{\mathbf{d}}$ collects displacements and rotation derivatives $\bar{\mathbf{d}} = \{\bar{\mathbf{u}}_{,s}, \bar{\mathbf{R}}_{,s}[\bar{\boldsymbol{\varphi}}]\}$, through a vector parametrization, the corotational relationships can be easily evaluated:

$$\bar{\mathbf{u}}_{,s} := \mathbf{Q}^T (\mathbf{e}_1 + \mathbf{u}_{,s}) - \mathbf{e}_1, \quad \bar{\mathbf{R}}_{,s}[\bar{\boldsymbol{\varphi}}] := \mathbf{Q}^T \mathbf{R}_{,s}[\boldsymbol{\varphi}] \quad (4)$$

The constitutive law becomes:

$$\mathbf{t} = \mathbf{H}^{-1} \boldsymbol{\varrho}[\bar{\mathbf{d}}] \quad (5)$$

Finally, ICM assumes rotation \mathbf{Q} defining the CR frame is fixed so that $|\bar{\mathbf{W}}| \ll 1$. A good compromise is to assume $\mathbf{Q} = \mathbf{R}[\varphi]$, thereby (4) become:

$$\bar{\mathbf{u}}_{,s} := \mathbf{R}^T[\varphi](\mathbf{e}_1 + \mathbf{u}_{,s}) - \mathbf{e}_1, \quad \bar{\mathbf{W}}[\bar{\varphi}]_{,s} := \mathbf{R}^T[\varphi]\mathbf{R}_{,s}[\varphi] \quad (6)$$

in which a linearization of rotations $\bar{\mathbf{R}}[\bar{\varphi}] = \mathbf{I} + \bar{\mathbf{W}}[\bar{\varphi}] + \dots$ is used.

2 IMPLICIT COROTATIONAL METHOD: FEM IMPLEMENTATION

The FEM implementation of the nonlinear model for beams and plates recovered using the ICM can be performed through different kinds of interpolation strategies [2].

In particular once obtained the continuum model for both Corotational (CR) or Total Lagrangian (TL) interpolations is obtained it could be easily used in a standard fashion to produce a discrete model suitable for use in asymptotic and path-following solution strategies.

2.1 General remarks

ICM allows the recovery of the mixed strain energy of the nonlinear model exploiting the kinematical relationship $\boldsymbol{\varrho}[\bar{\mathbf{d}}]$ in terms of kinematical parameters $\bar{\mathbf{d}}$ in the CR frame rotated by \mathbf{Q} :

$$\Phi[\mathbf{t}, \bar{\mathbf{d}}] = \int_s \left\{ \mathbf{t}^T \boldsymbol{\varrho}[\bar{\mathbf{d}}] - \frac{1}{2} \mathbf{t}^T \mathbf{H} \mathbf{t} \right\} ds \quad (7)$$

s being a suitable one or two dimensional abscissa. Using the geometrical relationships

$$\bar{\mathbf{d}} = \mathbf{g}[\mathbf{d}] \quad (8)$$

between kinematical parameters $\bar{\mathbf{d}}$ and the corresponding ones in global fixed frame \mathbf{d} , the strain energy (7) can be expressed in terms of \mathbf{d} :

$$\Phi[\mathbf{t}, \mathbf{d}] = \int_s \left\{ \mathbf{t}^T \boldsymbol{\varrho}[\mathbf{d}] - \frac{1}{2} \mathbf{t}^T \mathbf{H} \mathbf{t} \right\} ds \quad (9)$$

Assuming an interpolation of generalized stress field defined by

$$\mathbf{t} = \mathbf{D}_t[s] \mathbf{t}_e \quad (10)$$

the discrete form of the complementary energy becomes

$$\Phi_{ce}[\mathbf{t}_e] = \frac{1}{2} \mathbf{t}_e^T \mathbf{H}_e \mathbf{t}_e, \quad \mathbf{H}_e := \int_s \{ \mathbf{D}_t^T[s] \mathbf{H} \mathbf{D}_t[s] \} ds \quad (11)$$

$\mathbf{D}_t[s]$ being the operator collecting the interpolation functions and \mathbf{t}_e the vector collecting the element stress parameters. The discrete form of internal work \mathcal{W}_e can be obtained in a different way depending on the motion description used, CR or TL.

2.2 Corotational interpolation

In this case the interpolation is performed on kinematical parameters $\bar{\mathbf{d}}$ in the CR frame:

$$\bar{\mathbf{d}} = \bar{\mathbf{D}}_d[s] \bar{\mathbf{d}}_e \quad (12a)$$

$\bar{D}_d[s]$ being the operator collecting the interpolation functions and \bar{d}_e the kinematical CR parameters of the element. Substituting the interpolation (13b) into (8) and performing integration we obtain the following discrete energy

$$\mathcal{W}_e[\mathbf{t}_e, \boldsymbol{\varrho}] = \mathbf{t}_e^T \boldsymbol{\varrho}_e[\bar{\mathbf{d}}_e], \quad \boldsymbol{\varrho}_e[\bar{\mathbf{d}}_e] := \int_s \{ \mathbf{D}_t^T[s] \boldsymbol{\varrho}[\bar{D}_d[s] \bar{\mathbf{d}}_e] \} ds \quad (12b)$$

The interpolation is completed exploiting the geometrical transformation law

$$\bar{\mathbf{d}}_e = \mathbf{g}_e[\mathbf{d}_e] \quad (12c)$$

between discrete kinematical parameters $\bar{\mathbf{d}}_e$ in the CR frame and the corresponding ones in the global fixed frame \mathbf{d}_e .

The aim of CR description is then to transfer the problem nonlinearity of the problem from the kinematical relationships to the geometrical transformation contained in eq. (12c). As the frame indifference requirements guarantee 'a priori' in terms of the rotation \mathbf{Q} by the geometric laws eq.(12c) the interpolation matrix $\bar{D}_d[s]$ could be the same used for the corresponding linear FEM interpolation of the same model. Furthermore as in this context also the finite element kinematical descriptor $\bar{\mathbf{d}}_e$ is also small, the discrete strain measure $\boldsymbol{\varrho}[\bar{\mathbf{d}}_e]$ can be expanded using Taylor expansion (see [3] for further details), without any loss in accuracy. Usually linear or quadratic expansions are used in this respect while the improvement in of accuracy is demanded for a refinement of the finite element mesh that is to a local better evaluation of \mathbf{Q} . Note that:

- When $\bar{D}_d[s]$ is assumed to be the same as the linear finite element model, $\boldsymbol{\varrho}_e[\bar{\mathbf{d}}_e]$ is linearized in terms of $\bar{\mathbf{d}}_e$ we obtain the "standard" form of the CR formulation [4] that allows us obtain, in an easy way, a nonlinear finite element starting from the corresponding linear one.
- The evaluation of the CR frame could be not constant on the element and, for example, evaluated in a series of Gauss points for a better elimination of the mean rigid body motion. This requires the integral in eq. (7) and the geometric law (8) to be split.

2.3 Total Lagrangian interpolation

In this strategy we interpolate the global kinematical parameters \mathbf{d}

$$\mathbf{d}[s] = \mathbf{D}_d[s] \mathbf{d}_e \quad (13a)$$

$\mathbf{D}_d[s]$ and \mathbf{d}_e being the operator containing the interpolation functions and \mathbf{d}_e the vector collecting the finite element kinematical parameters. The energy (9) then becomes:

$$\mathcal{W}_e[\mathbf{t}_e, \boldsymbol{\varrho}_e] = \mathbf{t}_e^T \boldsymbol{\varrho}_e[\mathbf{d}_e], \quad \boldsymbol{\varrho}_e[\mathbf{d}_e] := \int_s \{ \mathbf{D}_t^T[s] \boldsymbol{\varrho}[\mathbf{D}_d[s] \mathbf{d}_e] \} ds \quad (13b)$$

In particular is well known (see [5] and references therein) that to obtain a frame indifferent model the finite element interpolation also needs to be frame indifferent so the choice of the interpolation functions contained in $\mathbf{D}_d[s]$ is in general important.

3 FEM IMPLEMENTATION FOR SAINT VENANT BEAM MODEL

In this section the 3D nonlinear beam model recovered from the Saint Venant general rod theory through ICM method and described in the paper [6] will be implemented here to obtain a nonlinear

element to be used within FEM analysis. The model account for shear deformability and for to the section warping due to the helicoid distortion due to torsion, i.e. the so-called Wagner effect. A separate (mixed) interpolation is used for section strengths $\mathbf{t}[s]$ and displacements $\mathbf{d}[s]$, s being a material abscissa along the beam axis.

3.1 Handling the nonlinear beam model

The beam model proposed into [6] is briefly summarized and handled. We consider a beam element, initially straight and of length ℓ , global strengths \mathbf{t} and strains $\boldsymbol{\varrho}$ are defined as

$$\mathbf{t} := [\mathbf{N}, \mathbf{M}]^T, \quad \boldsymbol{\varrho} = \boldsymbol{\varrho}_L + \boldsymbol{\varrho}_Q \quad (14a)$$

\mathbf{N} and \mathbf{M} being the vectors collecting axial/shear strengths and torsional/bending couples and

$$\boldsymbol{\varrho}_L = [\varepsilon_L, \chi_L]^T, \quad \boldsymbol{\varrho}_Q = \boldsymbol{\Psi}[\boldsymbol{\varrho}_L]\boldsymbol{\varrho}_L \quad (14b)$$

where ε_L and χ_L are defined by

$$\varepsilon_L := \mathbf{R}^T(\mathbf{u}_{,s} + \mathbf{e}_1) - \mathbf{e}_1, \quad \chi_L := \mathbf{T}^T\boldsymbol{\varphi}_{,s} \quad (14c)$$

as function of displacements $\mathbf{u}[s]$ and rotations $\boldsymbol{\varphi}[s]$ associated to a material abscissa s varying from 0 to ℓ , and matrix $\boldsymbol{\Psi}[\boldsymbol{\varrho}_L]$ defined into [6] account quadratic coupling (i.e. Wagner effect). Using Rodrigues parametrization matrix \mathbf{R} and \mathbf{T} can be expressed as

$$\mathbf{R}(\varphi) = \mathbf{I} + \frac{\sin \varphi}{\varphi} \mathbf{W}[\varphi] + \frac{(1 - \cos \varphi)}{\varphi^2} \mathbf{W}^2[\varphi], \quad \mathbf{T}[\varphi] = \mathbf{I} + \frac{1 - \cos \varphi}{\varphi^2} \mathbf{W}[\varphi] + \frac{\varphi - \sin \varphi}{\varphi^3} \mathbf{W}^2[\varphi]$$

Finally, the model is completed by compliance operator \mathbf{H} (see [6]), which is here split as

$$\mathbf{H} := \begin{bmatrix} \mathbf{H}_{nn} & \mathbf{H}_{nm} \\ \mathbf{H}_{nm}^T & \mathbf{H}_{mm} \end{bmatrix} \quad (15)$$

3.2 Mixed finite beam element

The finite element for the SV beam model assumes \mathbf{N} is constant and \mathbf{M} linear while displacements and rotations, to avoid locking, are interpolated independently. In particular for the local rotation vectors $\boldsymbol{\varphi}$, a quadratic interpolation is assumed while displacements $\bar{\mathbf{u}}$ are assumed as linear on the element. In the following quantities evaluated on the edge of the beam ($s = 0$ and $s = \ell$), will be denoted with the pedex i and j , while the average quantities will be denoted with the pedex m (for further details see [2]). Note that a Rodrigues parametrization for the rotation will be used in the sequel.

Introducing the symmetric and skew-symmetric couples \mathbf{m}_s and \mathbf{m}_e :

$$\mathbf{m}_s := -(\mathbf{M}_j + \mathbf{M}_i), \quad \mathbf{m}_e := (\mathbf{M}_j - \mathbf{M}_i) \quad (16a)$$

the constant interpolation for the axial-shear forces and the linear interpolation for bending and torsional moments becomes:

$$\mathbf{N} = \frac{\mathbf{n}_e}{l}, \quad \mathbf{M} = -\frac{1}{2}(\mathbf{m}_s + f_s \mathbf{m}_e) \quad (16b)$$

Letting $\mathbf{t}_e := \{\mathbf{n}_e, \mathbf{m}_s, \mathbf{m}_e\}$ the vector collecting the *natural stress* eq.(16b) becomes

$$\mathbf{N} = \mathbf{D}_n \mathbf{t}_e, \quad \mathbf{M} = \mathbf{D}_m \mathbf{t}_e \quad (16c)$$

with

$$\mathbf{D}_n := \frac{1}{l} [\mathbf{I}_3 \quad \mathbf{0}_3 \quad \mathbf{0}_3], \quad \mathbf{D}_m := \frac{1}{2} [\mathbf{0}_3 \quad -\mathbf{I}_3 \quad f_s \mathbf{I}_3] \quad (16d)$$

with \mathbf{I}_3 and $\mathbf{0}_3$ the identity and zero matrix in \mathbb{R}^3 and $f_s := 1 - 2\frac{s}{l}$.

Substituting stress interpolation (16) into complementary energy (11), the discrete complementary matrix \mathbf{H}_e then becomes

$$\mathbf{H}_e := \begin{bmatrix} \frac{1}{l} \mathbf{H}_{NN} & -\frac{1}{2l} \mathbf{H}_{NM} & \mathbf{0}_3 \\ -\frac{1}{2l} \mathbf{H}_{NM}^T & \frac{1}{4} \mathbf{H}_{MM} & \mathbf{0}_3 \\ \mathbf{0}_3 & \mathbf{0}_3 & \frac{l}{12} \mathbf{H}_{MM} \end{bmatrix} \quad (17)$$

As regards kinematics, the displacement and rotation vector field is assumed to be linear and quadratic on the element. Defining the vector $\bar{\mathbf{d}}_e := \{\bar{\phi}_r, \bar{\phi}_s, \bar{\phi}_e, \bar{\phi}_m\}$, collecting the *natural modes*:

$$\bar{\phi}_r := \frac{\bar{\mathbf{u}}_j - \bar{\mathbf{u}}_i}{l}, \quad \bar{\phi}_s := \frac{\bar{\varphi}_i - \bar{\varphi}_j}{2}, \quad \bar{\phi}_e := \frac{\bar{\varphi}_i + \bar{\varphi}_j}{2} - \bar{\phi}_m, \quad \bar{\phi}_m := \frac{1}{l} \int_0^l \bar{\varphi} ds \quad (18a)$$

the interpolation can be expressed as:

$$\bar{\mathbf{u}}_{,s} = \bar{\mathbf{D}}_u \bar{\mathbf{d}}_e, \quad \bar{\varphi} = \bar{\mathbf{D}}_\varphi \bar{\mathbf{d}}_e \quad (18b)$$

with

$$\bar{\mathbf{D}}_u := [\mathbf{I}_3 \quad \mathbf{0}_3 \quad \mathbf{0}_3 \quad \mathbf{0}_3], \quad \bar{\mathbf{D}}_\varphi := [\mathbf{0}_3 \quad f_s \mathbf{I}_3 \quad f_e \mathbf{I}_3 \quad \mathbf{I}_3] \quad (18c)$$

and interpolation function $f_e := 1 - 6\frac{s}{l} + 6\frac{s^2}{l^2}$. Substituting strength interpolation laws (16) into internal work (13b) with some algebra we have for finite strain

$$\rho_e[\bar{\mathbf{d}}_e] := [\bar{\phi}_r + \mathbf{W}_1 \bar{\phi}_m, \bar{\phi}_s, \bar{\phi}_e]^T, \quad \mathbf{W}_1 = \text{spin}(\mathbf{e}_1)$$

The element definition is completed by the geometrical relationship between corotational and fixed frame denoted with $\bar{\mathbf{d}}_e = \bar{\mathbf{g}}_e[\mathbf{d}_e]$ (see (12c)), that allows the recovery of $\boldsymbol{\varrho}_e[\mathbf{d}_e]$. Introducing $\mathbf{d}_e := \{\phi_r, \phi_s, \phi_e, \phi_m\}$, where

$$\phi_r := \frac{\mathbf{u}_j - \mathbf{u}_i}{l}, \quad \phi_s := \frac{\varphi_i - \varphi_j}{2}, \quad \phi_e := \frac{\varphi_i + \varphi_j}{2} - \phi_m, \quad \phi_m := \mathbf{Q}[\boldsymbol{\alpha}]^T \mathbf{R}[\phi_m]$$

and selecting CR frame so that $\boldsymbol{\alpha} \equiv \phi_m$ (that is $\bar{\phi}_m = 0$), we have for $\boldsymbol{\varrho}_e[\mathbf{d}_e]$

$$\boldsymbol{\varrho}_e[\mathbf{d}_e] := \begin{bmatrix} \mathbf{Q}^T(\phi_r + \mathbf{e}_1) - \mathbf{e}_1 \\ \frac{1}{2} (\log[\mathbf{Q}^T \mathbf{R}_i] - \log[\mathbf{Q}^T \mathbf{R}_j]) \\ \frac{1}{2} (\log[\mathbf{Q}^T \mathbf{R}_i] + \log[\mathbf{Q}^T \mathbf{R}_j]) \end{bmatrix} \quad (19)$$

with $\mathbf{Q} = \mathbf{R}(\phi_m)$, $\mathbf{R}_i = \mathbf{R}(\phi_e - \phi_s)$ and $\mathbf{R}_j = \mathbf{R}(\phi_e + \phi_s)$ and $\log[\cdot]$ standing for the extraction of the rotation vector from a rotation tensor (for further details on algebra and rotation handling see [2]). Finally note that, splitting rotation \mathbf{R} as

$$\mathbf{R}[\varphi] = \mathbf{Q}[\phi_m] \bar{\mathbf{R}}[\varphi]$$

and using for $\mathbf{u}_{,s}$ and $\bar{\varphi}$ the following interpolation

$$\mathbf{u}_{,s} = \bar{\mathbf{D}}_u \bar{\mathbf{d}}_e, \quad \bar{\varphi} = \bar{\mathbf{D}}_\varphi \bar{\mathbf{d}}_e, \quad \bar{\mathbf{D}}_u := [\mathbf{I}_3, \mathbf{0}_3, \mathbf{0}_3, \mathbf{0}_3], \quad \bar{\mathbf{D}}_\varphi := [\mathbf{0}_3, \mathbf{f}_s \mathbf{I}_3, \mathbf{f}_e \mathbf{I}_3, \mathbf{0}_3] \quad (20)$$

the evaluation of the energy (13b) gives for $\boldsymbol{\rho}_e[\bar{\mathbf{d}}_e]$ the same expression as the CR case (19). Finally note that the element can be improved as previously stated using a quadratic expression for local rotation strain (see [3]).

3.3 FEM implementation for plate model: some remarks

For the nonlinear plate model recovered using ICM a FEM implementation can be performed following the methodologies proposed for the non linear beam model. The details of the implementation can be found in [2], however an outline is given here.

The nonlinear plate has been implemented in an already available asymptotic code named **KASP** (see [7]), in order to perform the post-buckling analysis of plate assemblages. The previous version of the codes was based on a technical plate suitable for performing a nonlinear analysis of plate assemblages.

The discrete model is based on a HC finite element interpolation [8] that avoids the need to use 3D finite rotation parameters so giving a simple energy expression even when a TL interpolation is used.

4 NUMERICAL RESULTS

The numerical results are principally related to the Koiter asymptotic analysis of plate assemblages and of 3D beam this being the most sensitive context of analysis to the correctness of the structural model and of its finite element implementation. However path-following analysis results based on the same continuum and discrete model are also proposed to check the accuracy of the obtained results. The equilibrium paths are compared with analytical results when possible, with results obtained by other authors or with the equilibrium path recovered using the commercial code ABAQUS.

The proposed Kirchoff plate model results, in the following denoted with the symbol (*PM*) have also been compared with those obtained by the same code using the technical models *complete Green Lagrange (LC)* and the *simplified Green Lagrange (LS)*, previously implemented in [7] to which we refer readers for further details. The proposed 3D beam finite element, implemented into a FEM code named **COBE** (see [2]) has been tested for cross-shaped sections having shear and bending centers which are not coincident, under axial and shear forces. The evaluation of compliance operator \mathbf{H}_e needed for the recovery of the complementary energy has been done through FEM technique applied to the cross section domain (for further details see [9]).

The possibility of modeling the same structure as 3D beam or as plate assemblages make possible a comparison regarding the accuracy of the proposed formulation both at the continuum and FEM level.

4.1 Z-shaped section beam under axial/shear forces

The test is a cantilever beam with **Z**-shaped cross section, analyzed like the previous test for two load conditions. The first is an axial force applied at the edge of the beam and at the centroid of the cross section with a lateral imperfection $\epsilon\lambda$ (see fig. 1) while the second is a lateral force applied at the centroid of the edge of the beam (see fig. 2). The geometry and elastic modula are reported in figures (1) and (2).

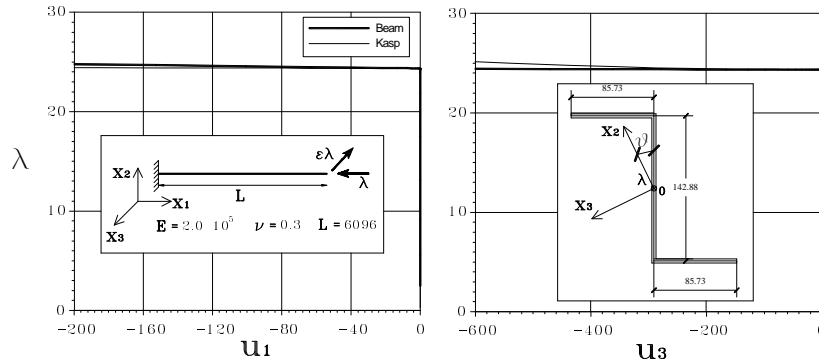


Figure 1: Z-shaped beam under axial force. Geometry and equilibrium paths.

For both load conditions, for the beam model 16 finite elements were used while for the plate model the mesh had 100 elements along the length of the cantilever beam and 5 elements for the wings and 10 for the web. The buckling occurs at $\lambda_b = 24.371$, for the axial force condition load, and is correctly and identically predicted by the beam and plate model, as in the previous test.

For the shear load case, there is some difference in the evaluation of the buckling load, for the same reasons as in the previous test. For the beam the buckling is predicted at $\lambda_b = 8.558$ while for the plate at $\lambda_b = 9.887$. The equilibrium paths are plotted for the axial and lateral displacements of the beam edge. The results obtained using the beam model agree well enough in the pre-critical and post-critical behavior with those recovered using **KASP** code.

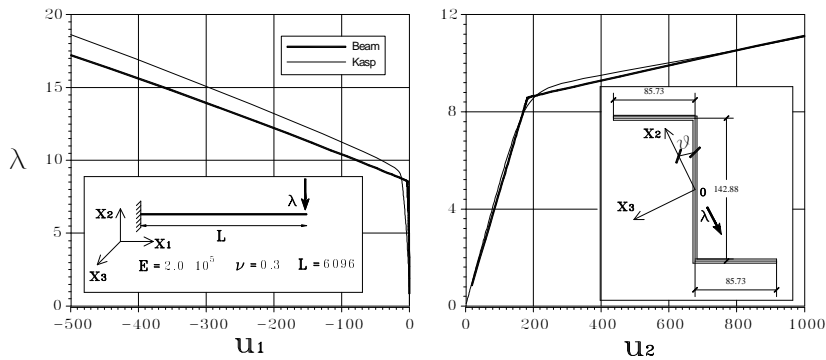


Figure 2: Z-shaped beam under shear force. Geometry and equilibrium paths.

4.1.1 C-shaped section beam

In the numerical analysis of the C-shaped section beam reported in fig.3 the good agreement between the numerical results obtained by the *PM* model in comparison with the path-following analysis performed by a co-rotational formulation proposed in [10] which is insensitive to the exact-

ness of the strain measures can be observed. As the critical mode is a torsional buckling the behavior of the plate assemblages is practically the same as a 3D beam. The buckling mode is not followed by stress redistribution and the postcritical curvature becomes very sensitive to the exactness of the strain model [10], as shown in fig. 4.

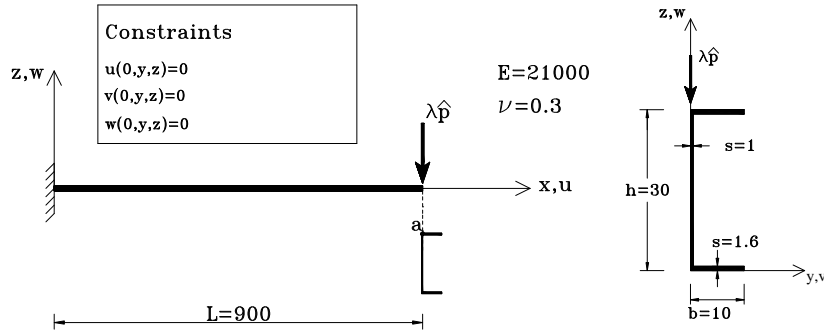


Figure 3: C section beam.

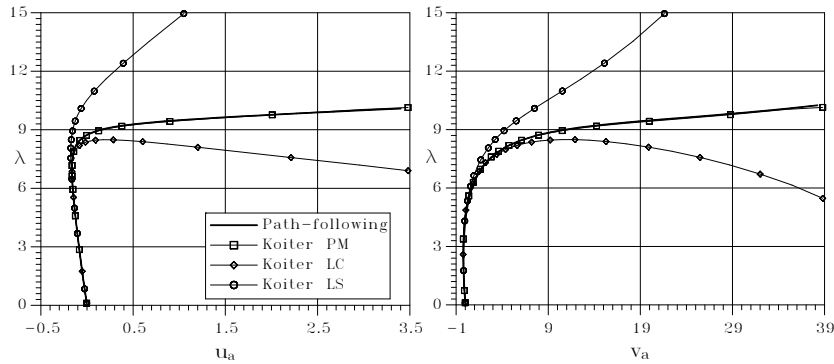


Figure 4: Cantilever C section beam: equilibrium paths.

5 CONCLUDING REMARKS

The suitability of the ICM for FEM implementation is a very strong point of the method. In fact, different kinds of interpolation (Total and Updated Lagrangian, Corotational) can be naturally placed within the approach.

A standard format to handle 3D rotation algebra and suitable for the implementation of ICM nonlinear models into path-following and asymptotic analyses has been proposed.

A FEM implementation is developed for both 3D beam and plate nonlinear model. In the former case a FEM code called **COBE** has been built aimed at both the path-following and asymptotic analyses of general spatial frame. In the latter case the proposed finite element has been implemented

as a specialized element into **KASP** code, already available at the University of Calabria and aimed at performing an asymptotic analysis of slender panel assemblages. A numerical investigation has been performed using both **COBE** and **KASP**. The numerical results always agree with the theoretical ones and the numerical benchmarks.

A good agreement is also found between the results obtained with the two different codes when applied to thin-walled beams. In conclusion ICM appears very promising, being suitable for application in different contexts and implementation in into FEM codes. Numerical simulations also confirm its potential and correctness.

References

- [1] G. Garcea, A. Madeo, 'Rational strain measures - The Implicit Corotational Method', ECCM - 2006 Lisbon.
- [2] A. Madeo, 'The Implicit Corotational Method: General theory and FEM implementation', Ph.d Thesis, University of Calabria, 2009. <http://www.labmec.unical.it/pubblicazioni/dottorato.php>.
- [3] G. Garcea, A. Madeo, G. Zagari, R. Casciaro, 'Asymptotic post-buckling FEM analysis using a corotational formulation', International Journal of Solids and Structures, Int. Journal of Solids & Structures **46** (2), 523-532, (2009).
- [4] C.C. Rankin, B. Nour-Omid, 'The use of projectors to improve finite element performance', Computer & Structures, **30**, pp. 257-267, (1988).
- [5] A. Ibrahimbegović, R. L. Taylor, 'On the role of frame-invariance in structural mechanics models at finite rotations', Computer Methods in Applied Mechanics and Engineering, **191**, pp. 5159-5176, (2002).
- [6] G. Garcea, A. Madeo, R. Casciaro, 'The implicit corotational method, Part I: Derivation of nonlinear structural models for beams and plates', Submitted to Computer Methods in Applied Mechanics and Engineering(2009).
- [7] G. Garcea, 'Mixed formulation in Koiter analysis of thin-walled beam', Computer Methods in Applied Mechanics and Engineering, **190**, pp. 3369-3399, (2001).
- [8] M. Aristodemo, 'A high-continuity finite element model for two-dimensional elastic problem', Computer & Structures, **21**, pp. 987-993, (1985).
- [9] A.S. Petrolo, R. Casciaro, '3D beam element based on Saint Venánt's rod theory', Computer & Structures, **82**, pp. 2471-2481, (2004).
- [10] G. Garcea, G.A. Trunfio, R. Casciaro, 'Path-following analysis of thin-walled structures and comparison with asymptotic post-critical solutions', Int. Journal for Numerical Methods in Engineering, **55**, pp. 73-100, (2002).